A Coupled Thermosphere-Exosphere Model: Results and Implications for Hydrogen Transport

Sarah Luettgen[1], Eric Sutton[2], Jeffrey Thayer[1]*

[1] Aerospace Engineering Sciences Department, University of Colorado at Boulder

[2] Space Weather Technology, Research & Education Center (SWx TREC), University of Colorado at Boulder

[*]Corresponding Author: sarah.luettgen@colorado.edu

I. Background and Objective

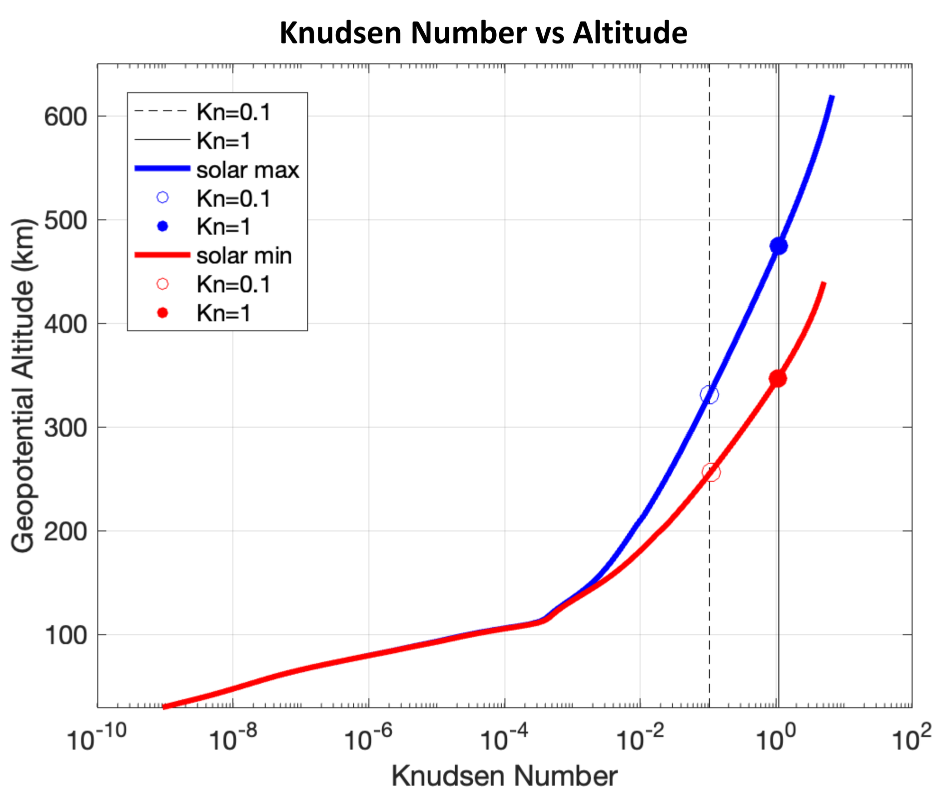

Fig 1. The Knudsen number, the ratio of the mean-free path to the atmospheric scale height, as a function of altitude for solar maximum (blue) and minimum (red).

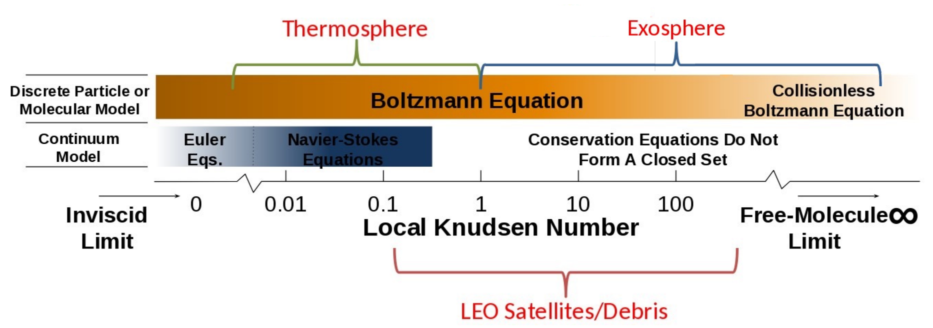

Fig 2. Knudsen number and associated validity of different solutions to the Boltzmann equation. Modified from [3].

Background:

- Ground to mid-thermosphere efficiently modeled using fluid equations in physical models, e.g., TIME-GCM
- Exosphere efficiently modeled using single-particle dynamics due to decrease in collisions

Problem:

- Assumptions used to simplify Boltzmann equation invalidated with increasing Knudsen number [3]

Kn = mean free path / atmospheric scale height

- Places limitation on altitude of TIME-GCM's upper boundary: ~300-600km
- Boundary conditions at exobase affect state of atmosphere lower down [1]

Solution: DSMC model

- DSMC model simulates exosphere
- Produce coupled model with smooth transition across exobase

Terms

- UB – upper boundary
- LB – lower boundary

II. Significance

- Model exobase flux without assumptions made in uncoupled TIME-GCM UB
- Quantify potential error in UB of common atmospheric model
- Visualize H transport in exosphere
- Extend UB of TIME-GCM without limitations imposed by decreasing Kn
- First simulations of exobase in equilibrium with thermospheric and exospheric thermal populations

III. Models

TIME-GCM [9]

- Fluid model
- Neutrals and thermal plasma
- LB = 32km
- UB ≈ 300-600km depending on solar input
  - Boundary condition:
    - Uncoupled model – analytic H escape flux
    - Coupled model – DSMC H flux
- Limitation: Physics
  - On UB due to increasing *Kn* near exobase

Monaco [4,10]

- DSMC model
- Neutrals only (H, He, O, N2)
- LB = 291km or 362km depending on solar input
  - Boundary conditions: set by TIME-GCM
- UB = 20,000km
  - Boundary condition: remove particle if reaches UB with $v > v_{esc}$, otherwise reflect downward
- Limitation: Computational
  - On LB due to computational expense
  - On UB due to exponential decrease in simulation particles with altitude

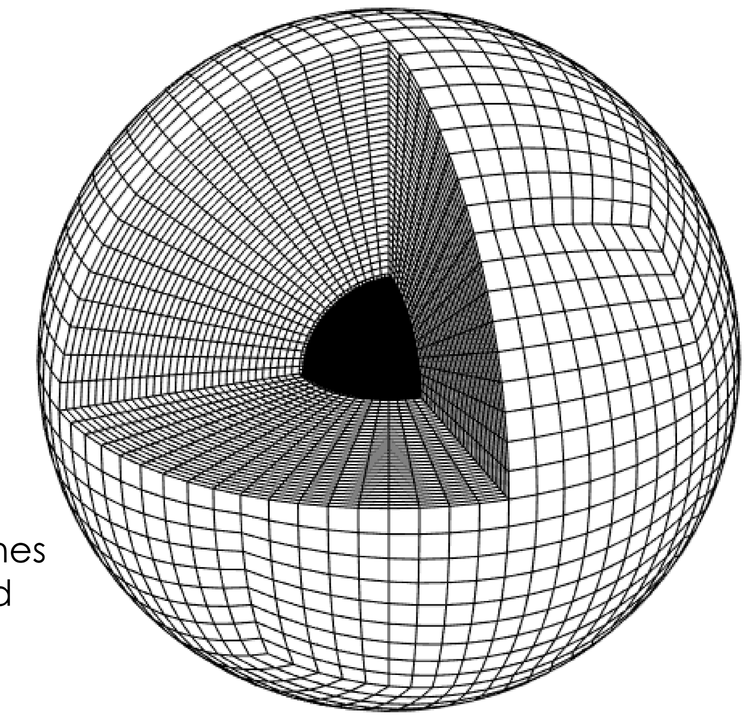

Fig 3. A "cubed-sphere" grid forms each layer of cells [11].

IV. Coupling

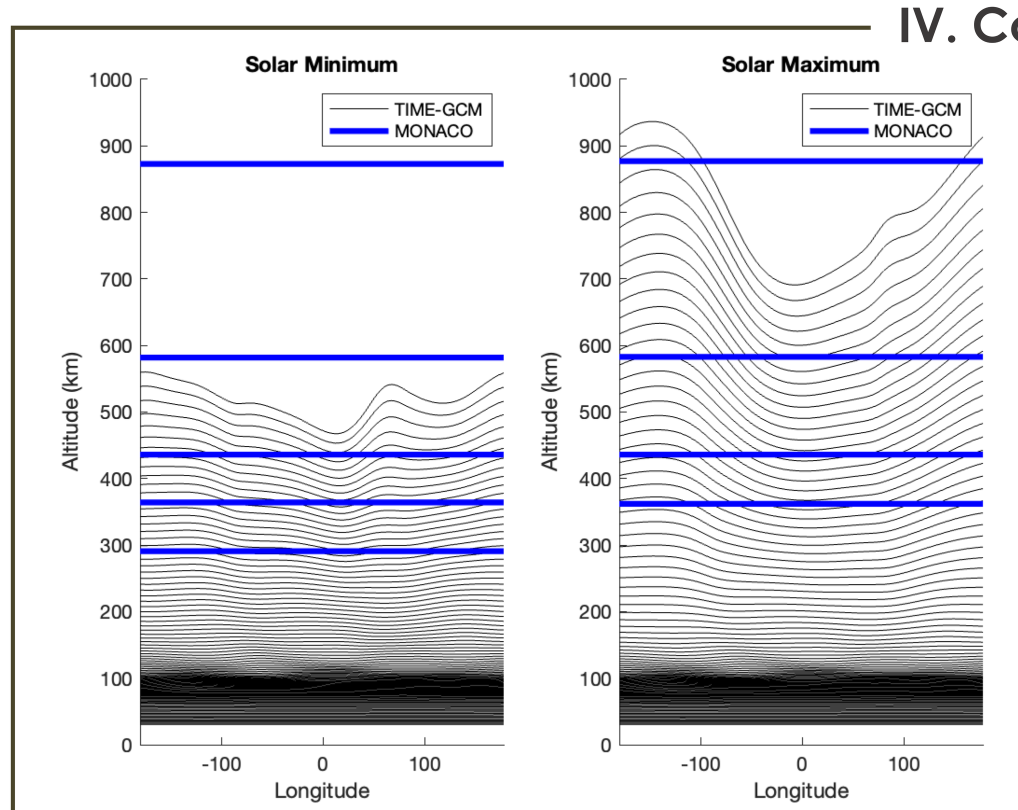

Fig 4. Vertical grids for TIME-GCM and Monaco from 0-1000 km; upper levels of Monaco not shown

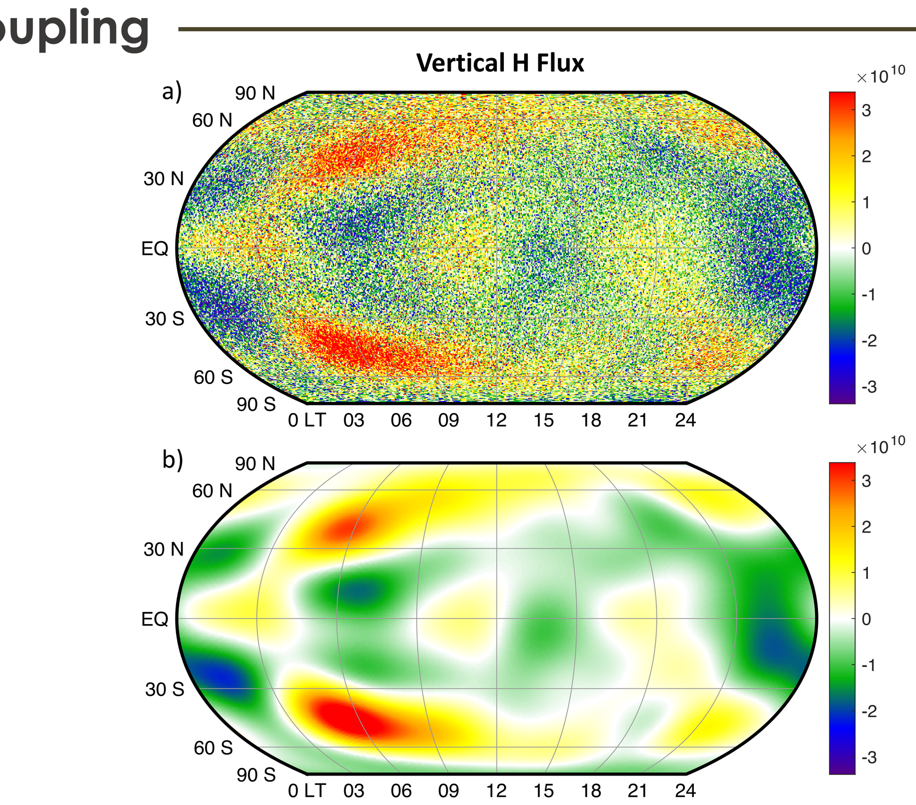

Fig 5. Upward flux of H through Monaco lower boundary (a) integrated over 10 minutes and (b) with spherical harmonic expansion. Presented with permission from [11].

Procedure [11] **:**

Monaco lower boundary

- Receive wind, temperature, densities from TIME-GCM
- Produce simulation particles with velocities randomly drawn from Maxwellian distribution
- Allow particles to propagate

TIME-GCM upper boundary

- Receive H flux from Monaco
- Perform spherical harmonic expansion on flux (see fig. 5)
- Interpolate H flux to TIME-GCM UB

V. Findings: H Transport in Exosphere

Solstice: three distinct, competing hydrogen circulation / transport regions observed.
Simulation for June Solstice, solar minimum.

Middle exosphere

- Single particle motion
- High temperature in summer hemisphere → energizes H atoms for higher and longer ballistic trajectories
- Transference of H to winter hemisphere

Lower exosphere

- Single particle motion
- High density in winter hemisphere → net ballistic motion up and away [8,12]
- Transference of H to summer hemisphere

Thermosphere [10]

- Continuum mechanics, use mass continuity principals
- Divergence in summer hemisphere → upward motion
- Convergence in winder hemisphere → downward motion and H accumulation

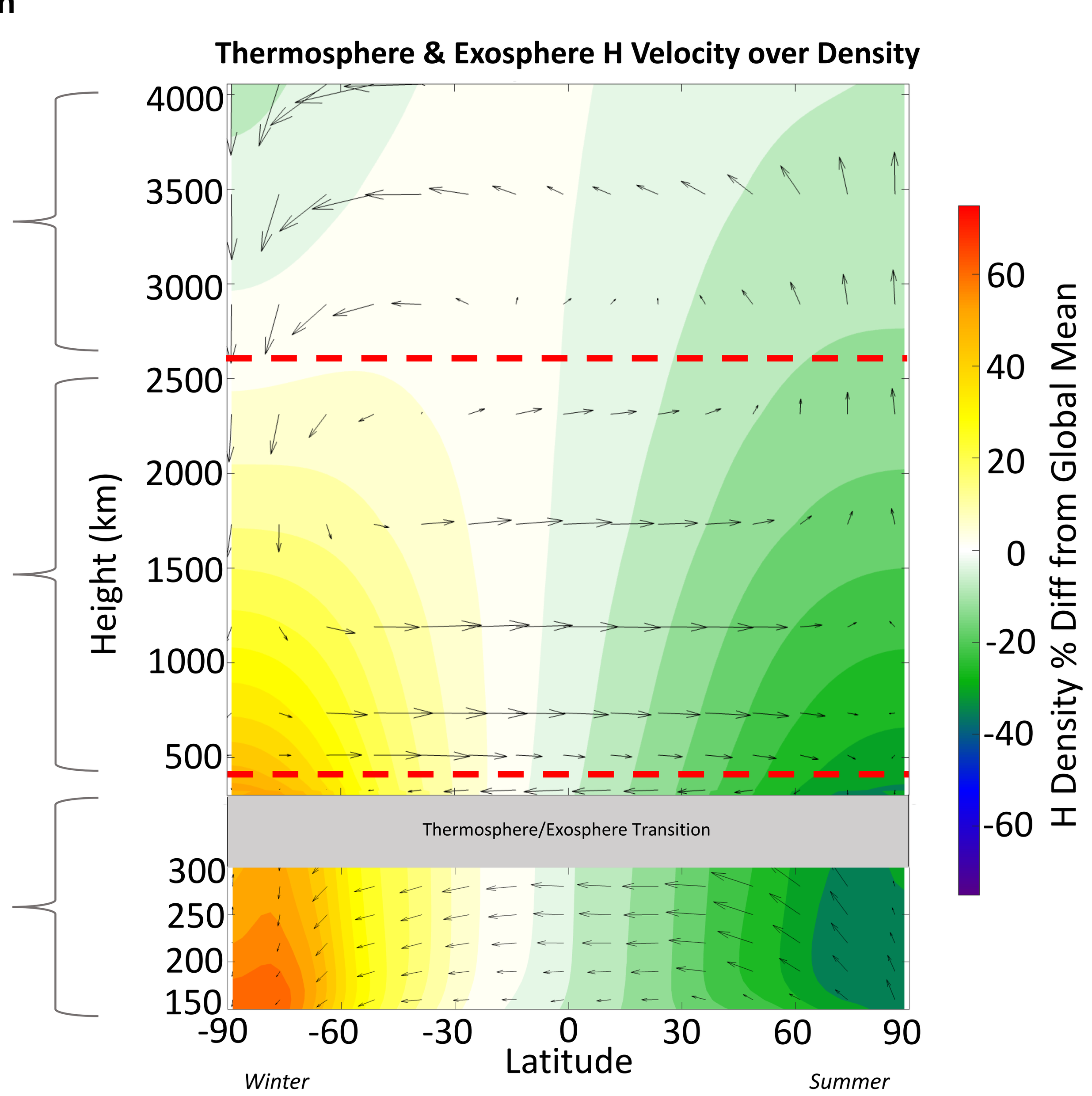

Fig 6. June solstice run. Quiver plot of H velocities over contour plot of H density percent difference from global mean. Red dashed lines separate left/right directionality of H velocity.

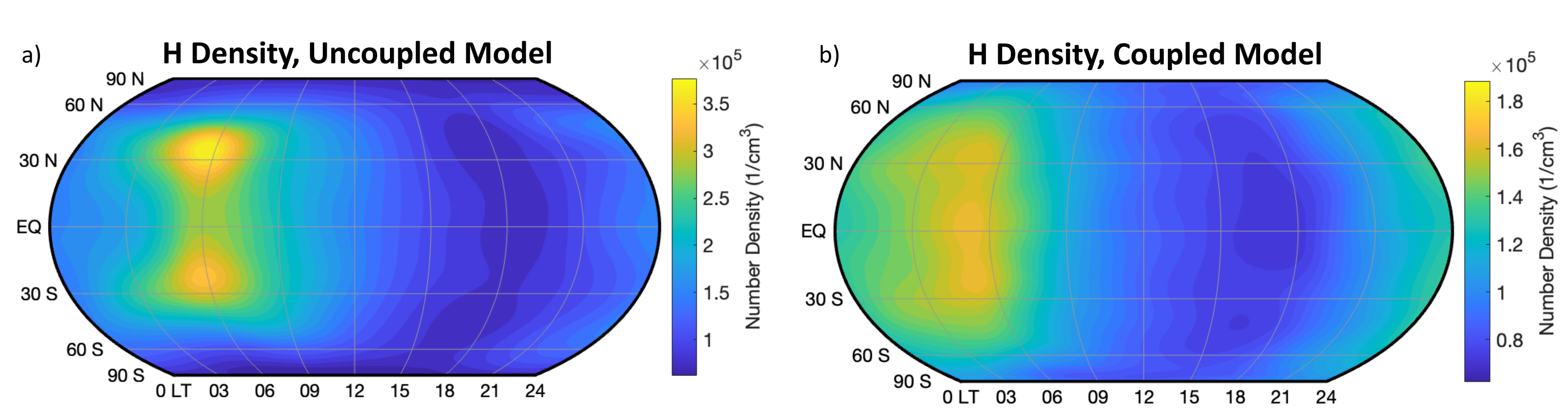

Thermospheric Density

- Horizontal dispersion of H due to lateral ballistic motion in exosphere

Fig 7. Density of H at 400 km during solar max, march equinox for the (a) uncoupled model and (b) coupled model. Color bar upper limit for (b) is half that of (a).

VI. Findings: Thermospheric Density Changes

Solar Max

- H number density decreases by 28%
- UB H flux out of model the same between coupled and uncoupled models
- Primary escape mechanism on Earth: thermal [2]

Solar Min

- H number density increases by 32%
- UB H flux out of model decreases by 12%
- Primary escape mechanism on Earth: non-thermal [2]

Current model only allows for thermal escape.

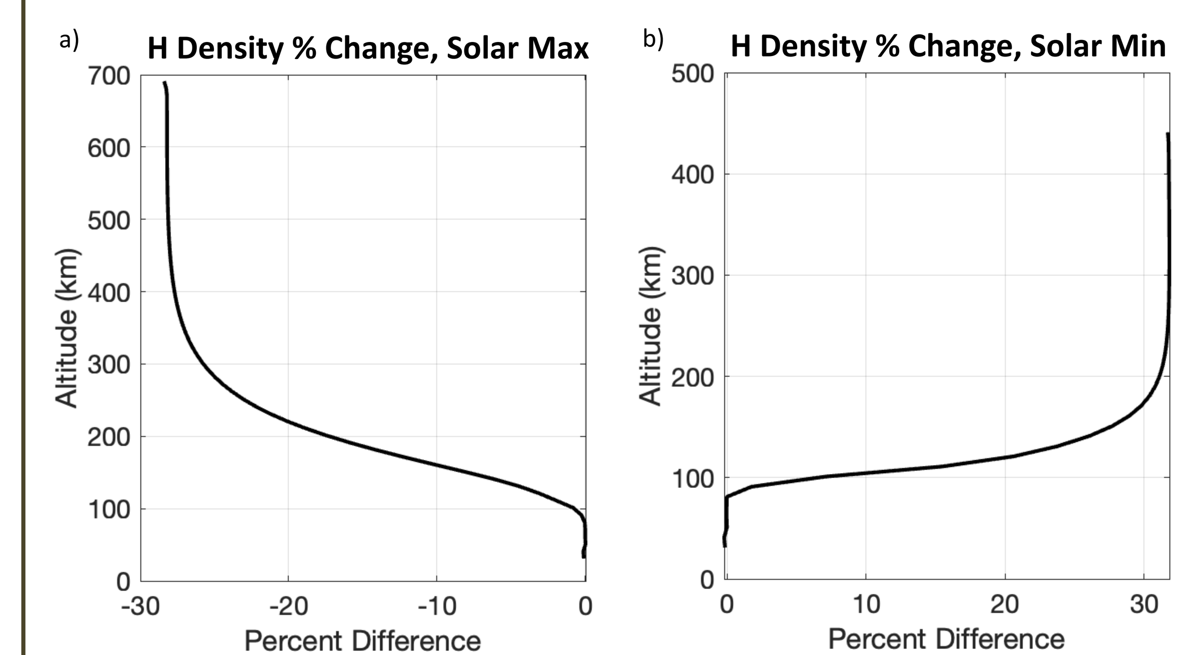

Fig 8. Percent difference in coupled model H density compared to uncoupled model for (a) solar maximum and (b) solar minimum.

VII. Future Steps: IPE

- Charged particle interactions with H are important to exospheric dynamics [6]
- Charge exchange interactions for H with H+ and O+ are consequential [5]
- The Ionosphere-Plasmasphere-Electrodynamics model (IPE) is a time-dependent, 3D ionosphere/plasmasphere model [7]
- Ion temperature and densities from IPE will be used to model charge exchange
- H escape and density are expected to be altered, particularly for solar minimum

VIII. Acknowledgements

The Authors would like to thank Professor Iain Boyd's research group for the development of the DSMC model Monaco, and the NASA HTMS and FINESST Programs for funding support.

Funding : NASA FINESST Proposal #20-HELIO20-0005
NASA HTMS Grant #80NSSC20K1278

IX. References

[1] Banks, P. and Kockarts, G. (1973). *Aeronomy*. Academic Press. doi: 10.1016/C2013-0-10329-7.

[2 Bertaux, J. L. (1975). Observed variations of the exospheric hydrogen density with the exospheric temperature, *J. Geophys. Res.*, 80(4), 639–642, doi:10.1029/JA080i004p00639.

[3] Bird, G. (1994). *Molecular Gas Dynamics and the Direct Simulation of Gas Flows*. Claredon Press. ISBN: 0198561954

[4] Boyd, I. and Schwartzentruber, T. (2017). *Nonequilibrium Gas Dynamics and Molecular Simulation*. Cambridge University Press. doi: 10.1017/9781139683494.

[5] Hodges, R. (1994). Monte Carlo Simulation of the Terrestrial Hydrogen Exosphere, *J. Geophys. Res.*, 99(A12), 23229–23247. doi:10.1029/94JA02183.

[6] Krall, J. et al. (2018). The Unknown Hydrogen Exosphere: Space Weather Implications. *Space Weather,* 16(3), 205–15. doi:10.1002/2017SW001780.

[7] Maruyama, N. et al. (2016). A New Source of the Midlatitude Ionospheric Peak Density Structure Revealed by a New Ionosphere-Plasmasphere Model. *Geophys. Res. Lett.,* 43(6), 2429–35. doi:10.1002/2015GL067312.

[8] McAfee, J.R. (1967). Lateral flow in the exosphere, *Planetary and Space Science*, 15(4), 599-609. doi: 10.1016/0032-0633(67)90033-5.

[9] Roble, R. G., and Ridley, E. C. (1994). A thermosphere-ionosphere-mesosphere-electrodynamics general circulation model (timeGCM): Equinox solar cycle minimum simulations (30–500 km), *Geophys. Res. Lett.*, 21(6), 417–420. doi: 10.1029/93GL03391

[10] Sutton, E. K. (2016). Interhemispheric transport of light neutral species in the thermosphere, *Geophys. Res. Lett.,* 43, 12,325–12,332. doi:10.1002/2016GL071679.

[11] Sutton, E. K. et al. (2023-in prep). Simulations of Hydrogen Transport through the Coupled Lower Exosphere-Thermosphere-Mesosphere System.

[12] Tinsley, B. A. (1973). The diurnal variation of atomic hydrogen, *Planetary and Space Science*, 21(4), 686-691. doi:10.1016/0032-0633(73)90080-9.